**EXAMINING THE EXTREME PETROFABRICS OF THE ORDINARY CHONDRITE IMPACT MELT ROCKS LAPAZ ICEFIELD 031125 AND LARKMAN NUNATAK 06299.** D. N. Jetoo[1], L. C. Malecek[1], J. M. Friedrich[1,2] and M. L. Rivers[3], [1]Department of Chemistry, Fordham University, Bronx, NY 10458 USA, [2]Department of Earth and Planetary Sciences, American Museum of Natural History, New York, NY 10024 USA (friedrich@fordham.edu), [3]Consortium for Advanced Radiation Sources, University of Chicago, Argonne, IL 60439 USA.

**Introduction:** Impacts involving chondritic parent bodies produce a variety of recognizable petrofabrics in meteorites. Low-intensity impacts have been hypothesized as the origin of petrofabrics in CM chondrites [1]. Increasing impact intensity correlates with increasing degrees of petrofabric anisotropy in ordinary chondrites [2-4]. High-intensity impact events can deposit sufficient energy to melt or even vaporize the rocks involved [e.g. 5]; however, such impact processes are notoriously chaotic, complex, and inhomogeneous. Little is known about the petrofabrics of the resulting impact melt rocks. In this work, we examine the three-dimensional (3D) petrofabrics of ordinary chondrite impact melt rocks using x-ray computed microtomography (μCT).

**Sample Background:** LaPaz Icefield (LAP) 031125 is an H chondrite impact melt rock that consists of a single rapidly-cooled lithology containing entrained metal (Fig. 1). The metal is rimmed by troilite [6]. Wittmann et al. [5] and Swindle et al. [6] demonstrated that LAP 031125 is a solidified impact melt with an Ar-Ar age date of 3942 ± 23 Ma. Wittmann et al. [5] hypothesized that LAP 031125 originated in an environment allowing radiation-dominated cooling, such as near the surface of an asteroid as a melt volume in a simple crater.

Larkman Nunatak (LAR) 06299 is an LL chondrite impact melt breccia consisting of two different lithologies: a vesicular melt rock (Fig. 1) and unmelted LL6 chondritic clasts [7]. The melt matrix lithology consists of metal-sulfide nodules often associated with vesicles (Fig. 1). Rubin and Moore [7] reported the chondritic clasts possess an S4 shock stage [8]. They [7] also concluded the relative orientations of metal-sulfide nodules and their associated vesicles indicate the gravitational orientation of LAR 06299 on the LL parent asteroid, with the metal-sulfide nodules indicating the gravitational "down" on the parent asteroid.

**Methods and Samples:** We imaged the samples using synchrotron x-ray computed microtomography (μCT) at the GSECARS 13-BMD beamline at the Advanced Photon Source of Argonne National Laboratory. We used monochromatic x-rays of 45.3 keV. We examined two fragments of LAR 06299,28 (336.5 and 267.8 mg) and a 456.23 mg fragment of LAR 06299,29, each at a resolution of 3.7 μm/voxel. Subsample ,28 is an example of the vesicular impact melt (as seen in Fig. 1) while the ,29 subsample is from the unmelted chondritic clast material. We imaged a 478.7 mg sample of LAP 031125 with a resolution of 5.7 μm/voxel. We used previously-published digital data extraction techniques [see 3,9] to examine the petrofabrics [10-12] and the 3D petrography of the samples.

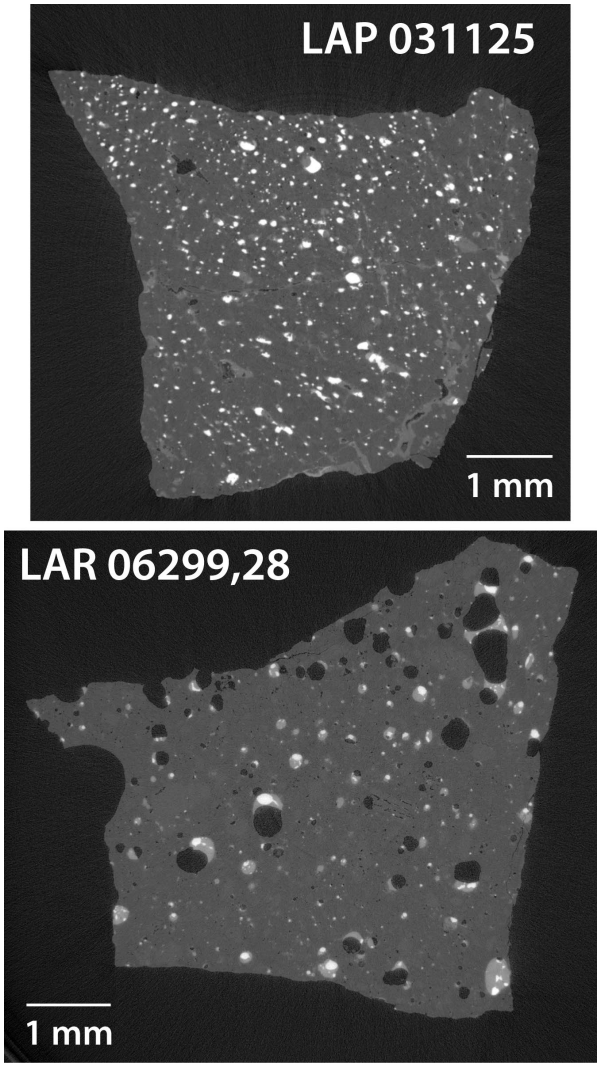


**Figure. 1.** X-ray tomograms of two impact melt rocks. Higher atomic weight materials are indicated by brighter grayscale values. The Fe–Ni metal grains and moderate grey FeS can easily be distinguished from the darker silicate materials. The black-colored vesicles in LAR can also be readily distinguished.

**Results and Discussion:**

*LAP 031125.* The petrofabric of LAP 031125, as defined by the metal globules, is defined by an overall planar ellipsoid (foliation). It is the most anisotropic foliation observed to date with our techniques in chondrites (Fig. 2). We interpret the fabric of LAP 031125 to be the result of the extreme uniaxial compression experienced by a melt sheet which subsequently rapidly solidified during near-surface cooling, akin to that hypothesized by [5]. Finally, we found a bulk density of 3.53 g/cm$^3$, which is reasonable for an H chondrite.

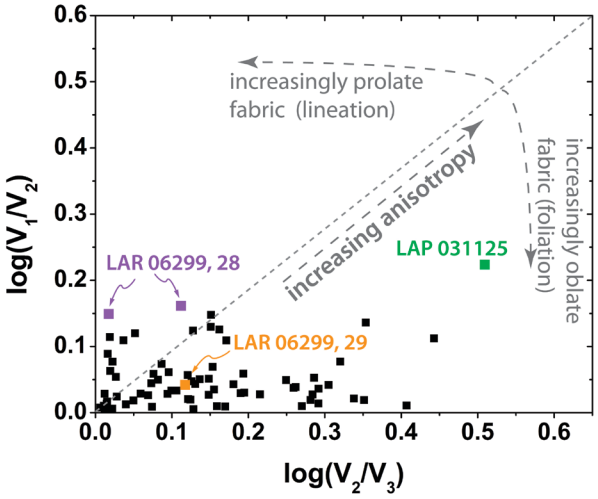


**Figure 2.** Ramsay-type plot [12, also see 10] illustrating the positions of the logs of ratios of fabric tensor eigenvalues for LAP 031125 and LAR 06299 samples. Such data give information on the type (foliation vs. lineation) and anisotropy of the petrofabrics. Comparison is made against ordinary chondrite petrofabric shape data (black squares) from [3,9,13-23].

*LAR 06299,28.* The petrofabric of LAR 06299,28, as defined by the orientations of the metal + sulfide + gas bubbles which were considered as one petrographic unit, consists of an unusual and prominent lineation. It is the clearest (most anisotropic) lineation observed to date (Fig. 2). Lineations in ordinary chondrites are uncommon (Fig. 2), with impact-related foliation being the norm [2, 3, 9]. Qualitatively, in 3D, the vesicles of LAR 06299,28 are nearly always associated with metal and sulfide assemblages and the sulfides are in contact with the vesicles. A cursory examination of the metal + sulfide + gas bubble relationships seem to concur with the findings of [7]. The lineation fabric of the ,28 lithology likely indicates injection or shear stress rather than a compaction.

*LAR 06299,29.* The chondritic portion (,29, not shown in Fig. 1) has a petrofabric defined by girdle major axis and a cluster minor axis, which indicates a foliation petrofabric. The anisotropy of the oblate foliation petrofabric is consistent with an S4 shock stage ordinary chondrite (Fig. 2). The bulk density of LAR 06299,29 is 3.37 g/cm$^3$.

**Conclusions:** LAP 031125 displays the most anisotropic planar petrofabric observed in chondrites with our techniques. The petrofabric of LAR 06299,28 consists of an unusual and extremely prominent lineation. The petrofabric of LAR 06299,29 consists of a foliation petrofabric with an anisotropy agreeing with an S4 petrofabric shock stage. Rapidly-cooled impact melt rocks retain a petrofabric record of their deformation.

**Acknowledgments:** US Antarctic meteorite samples are recovered by ANSMET and characterized and curated by the Smithsonian Institution and NASA Johnson Space Center. Portions of this work were performed at GeoSoilEnviroCARS (The University of Chicago, Sector 13), Advanced Photon Source (APS), Argonne National Laboratory.

**References:** [1] Lindgren P. et al. (2015) *Geochim. Cosmochim. Acta, 148*, 159–178. [2] Gattacceca J. et al. (2005) *Earth. Planet. Sci. Lett. 234*, 351–368. [3] Friedrich et al. (2008) *Earth. Planet. Sci. Lett. 275*, 172–180. [4] Miyahara M. et al. (2021) *J. Geophys. Res. Planet, 126*, e2021JE006864. [5] Wittmann A. et al. (2010) *J. Geophys. Res., 115*, E07009. [6] Swindle T. D. et al. (2009) *Meteoritics & Planet. Sci., 44,* 747–762. [7] Rubin A. E. and Moore W. B. (2011) *Meteoritics & Planet. Sci., 46,* 737–747. [8] Stöffler D. et al. (2018) *Meteoritics & Planet. Sci., 53,* 5–49. [9] Friedrich et al. (2017) *Geochim. Cosmochim. Acta, 203*, 157–174. [10] Woodcock N. H. (1977) *Geo. Soc. Am. Bull., 88*, 1231–1236. [11] Woodcock N. H. and Naylor M. A. (1983) *J. Struct. Geo. 5*, 539–549. [12] Ramsay J. G. (1967) *Folding and Fracturing of Rock.* McGraw-Hill, NY. [13] Friedrich J. M. (2008) *Comp. & Geosci., 34*, 1926–1935. [14] Friedrich et al. (2008) *Planet. Space. Sci., 56*, 895–900. [15] Sasso M. R. (2009) *Meteoritics & Planet. Sci., 44,* 1743–1753. [16] Friedrich J. M. and Rivers M. L. (2013) *Geochim. Cosmochim. Acta, 116*, 63–70. [17] Popova O. P. et al. (2013) *Science. 234*, 1069-1073. [18] Friedrich et al. (2014) *Meteoritics & Planet. Sci., 49,* 1214–1231. [19] Jenniskens P. et al. (2014) *Meteoritics & Planet. Sci., 49,* 1388–1425. [20] Dyl K. A. et al. (2016) *Meteoritics & Planet. Sci., 51,* 596–613. [21] Ruzicka A. M. et al. (2017) *Meteoritics & Planet. Sci., 52,* 1963–1990. [22] Friedrich et al. (2017) *Geochim. Cosmochim. Acta, 203*, 157–174. [23] Anderson S. et al. (2021) *Meteoritics & Planet. Sci., 56,* 241–259.